Spectral spatial coherence of high-power multi-chip LEDs*

CHEN Guang-ming(陈光明)[1,2], **TAO Hua**(陶华)[1], **LIN Hui-chuan**(林惠川)[1], **CHEN Zi-yang**(陈子阳)[1], and **PU Ji-xiong**(蒲继雄)[1**]

1. College of Information Science & Engineering, Huaqiao University, Xiamen 361021, China

2. Fujian Institute of Education, Fuzhou 350025, China

(Received 18 August 2012)

We investigate the spatial coherence of the light generated from high-power multi-chip red LEDs by using the van Cittert-Zernike theorem. It is theoretically demonstrated that the light generated from multi-chip LEDs evolves into partially coherent light after propagation, and the spatial coherence is increased with the increase of propagation distance. Moreover, the spatial coherence of the light is found to be closely related to the chip distribution of multi-chip LEDs. The distribution of the spatial coherence of the light is experimentally examined by Young's double-slit interference. It is found that the experimental results are consistent with the theoretical ones.

Document code: A **Article ID:** 1673-1905(2012)06-0422-4

DOI 10.1007/s11801-012-2322-6

The investigations of spectral characteristics on LEDs are mainly focused on the fields of spectral peak, spectral width and color temperature[1-9]. Few studies have been done on the coherence characteristics of the light generated from LEDs[10-13]. Recently, Mehta and his colleagues[14] reported the measurement of coherence characteristics of low-power single-color LEDs. With the development of LED chip manufacturing process and packaging technology, the lifetime of high-power and high-brightness LEDs is gradually extended[3-13]. However, to the best of our knowledge, as a kind of widely used light source, there is no paper studying the coherence of the light generated from high-power multi-chip red LEDs. In this paper, we study the spatial coherence of two different types of high-power multi-chip LEDs theoretically and experimentally. It is found that the light generated from incoherent light source evolves into the partially coherent light after propagation, and its spatial coherence is related to the chip distribution of multi-chip LEDs. The experimental results obtained by double-slit interference are consistent with the theoretical ones.

As shown in Fig.1, two different types of high-power multi-chip red LEDs are employed in our experiment, in which the small black squares in the middle of the LEDs indicate the light-emitting areas. Fig.1(a) presents a 2×2 chip LED, and Fig.1(b) shows a 4 × 5 chip LED.

According to van Cittert-Zernike theorem, the spatial coherence of the light generated from a quasi-monochromatic

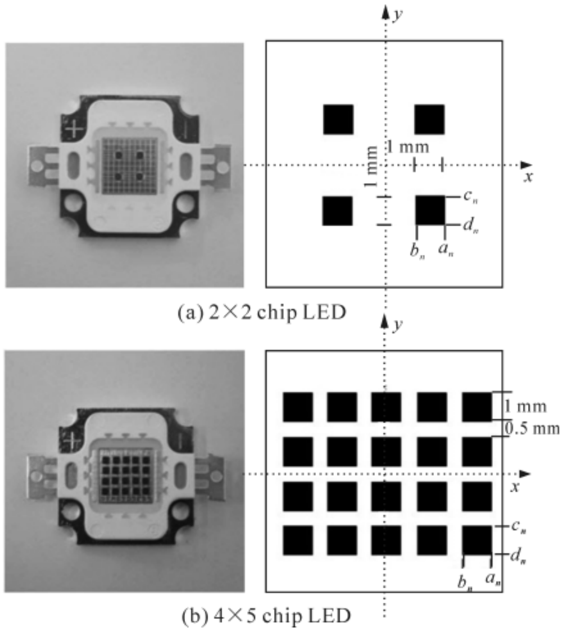

Fig.1 Schematic diagrams of high-power multi-chip LEDs

incoherent light source can change after propagation. In the paraxial approximation condition, the spatial coherence can be expressed as[15-17]

$$\mu_{12}(x_2-x_1, y_2-y_1, z) = \exp(\mathrm{i}\alpha_{12})\times \frac{\iint_S I(x,y)\exp[-\mathrm{i}\,2\pi(px+qy)]\,\mathrm{d}x\,\mathrm{d}y}{\iint_S I(x,y)\,\mathrm{d}x\,\mathrm{d}y}, \tag{1}$$

* This work has been supported by the National Natural Science Foundation of China (Nos.60977068 and 61178015).

** E-mail: jixiong@hqu.edu.cn

where $\alpha_{12} = 2\pi \frac{(x_2^2 + y_2^2) - (x_1^2 + y_1^2)}{2\lambda z}$, $p = \frac{x_2 - x_1}{\lambda z}$, $q = \frac{y_2 - y_1}{\lambda z}$, z is the distance between the light source and the observation plane, λ is the peak wavelength of quasi-monochromatic incoherent light, and $I(x, y)$ is the light intensity distribution of the source, which is supposed to be independent of the position, i.e., $I(x, y) = I_0$. The spatial coherence of the multi-chip LED light source can be obtained by solving the integral shown in Eq.(1). Based on van Cittert-Zernike theorem, the spatial coherence of the light generated from the multi-chip LEDs is given by following expression:

$$\mu_{12}(x_2 - x_1, y_2 - y_1, z) = \sum_{n=1}^{N} \frac{1}{I_0(\int_{b_n}^{a_n}\int_{d_n}^{c_n} \mathrm{d}x\,\mathrm{d}y)} \times \int_{b_n}^{a_n}\int_{d_n}^{c_n} \frac{I_0}{z^2} \exp\left\{\frac{\mathrm{i}k}{2z}[(x_2^2 + y_2^2) - (x_1^2 + y_1^2)] + \frac{\mathrm{i}k}{z}(x_2 - x_1)x + \frac{\mathrm{i}k}{z}(y_2 - y_1)y\right\} \mathrm{d}x\,\mathrm{d}y , \quad (2)$$

where N is the number of the small square light-emitting areas. $b_n < x < a_n$ represents the coordinates range of the nth small square light-emitting area along x direction, and $d_n < y < c_n$ represents the coordinates range of the nth small square light-emitting area along y direction. By solving the integral shown in Eq.(2), we obtain

$$\mu_{12}(x_2 - x_1, y_2 - y_1, z) = \sum_{n=1}^{N} \frac{-\lambda^2 z^2 \exp\left\{\frac{\pi[(x_2^2 + y_2^2) - (x_1^2 + y_1^2)]\mathrm{i}}{\lambda z}\right\}}{4\pi^2 N(x_2 - x_1)(y_2 - y_1)(a_n - b_n)(c_n - d_n)} \times \left\{\exp\left[\frac{-2\pi a_n(x_2 - x_1)\mathrm{i}}{\lambda z}\right] - \exp\left[\frac{-2\pi b_n(x_2 - x_1)\mathrm{i}}{\lambda z}\right]\right\} \times \left\{\exp\left[\frac{-2\pi c_n(y_2 - y_1)\mathrm{i}}{\lambda z}\right] - \exp\left[\frac{-2\pi d_n(y_2 - y_1)\mathrm{i}}{\lambda z}\right]\right\} . \quad (3)$$

It is shown from Eq.(3) that the light field at z observation plane is partially coherent, which indicates that the light generated from incoherent spontaneous emission multi-chip LED light source can change to partially coherent light after propagation in free space, and the spatial coherence can increase with the increase of the propagation distance.

Setting $x_1 = 0$ and $y_1 = 0$, we can rewrite Eq.(3) as

$$\mu_{12}(x_2, y_2, z) = \sum_{n=1}^{N} \frac{-\lambda^2 z^2 \exp\left[\frac{\pi(x_2^2 + y_2^2)\mathrm{i}}{\lambda z}\right]\left\{\exp\left[\frac{-2\pi a_n x_2 \mathrm{i}}{\lambda z}\right] - \exp\left[\frac{-2\pi b_n x_2 \mathrm{i}}{\lambda z}\right]\right\}}{4\pi^2 N x_2 y_2 (a_n - b_n)(c_n - d_n)} \times \left\{\exp\left[\frac{-2\pi c_n y_2 \mathrm{i}}{\lambda z}\right] - \exp\left[\frac{-2\pi d_n y_2 \mathrm{i}}{\lambda z}\right]\right\} . \quad (4)$$

By taking $x_2 = \rho_2\cos\theta$ and $y_2 = \rho_2 \sin\theta$, the spatial coherence can be expressed as

$$\mu_{12}(\rho_2, \theta, z) = \sum_{n=1}^{N} \frac{-\lambda^2 z^2 \exp\left[\frac{\pi\rho_2^2 \mathrm{i}}{\lambda z}\right]\left\{\exp\left[\frac{-2\pi \mathrm{i} a_n \rho_2 \cos\theta}{\lambda z}\right] - \exp\left[\frac{-2\pi \mathrm{i} b_n \rho_2 \cos\theta}{\lambda z}\right]\right\}}{4\pi^2 N\rho_2^2 \sin\theta\cos\theta(a_n - b_n)(c_n - d_n)} \times \left\{\exp\left[\frac{-2\pi \mathrm{i} c_n \rho_2 \sin\theta}{\lambda z}\right] - \exp\left[\frac{-2\pi \mathrm{i} d_n \rho_2 \sin\theta}{\lambda z}\right]\right\} . \quad (5)$$

The central wavelength of the multi-chip LEDs is λ=625 nm. The distribution of the spatial coherence of the light from two different types of multi-chip LEDs with different propagation distances can be obtained by numerically solving the integral shown in Eqs.(4) and (5). The numerical calculation results are presented in Figs.2 and 3, which show that the light generated from the incoherent multi-chip LEDs evolves into the partially coherent light after propagation, and the spatial coherence increases with increase of the propagation distance. Moreover, it is shown that by comparing the different spatial coherence distributions in Figs.2 and 3, the distribution of the spatial coherence of the light generated from the multi-chip LEDs is closely related to the chip distribution of the multi-chip LEDs.

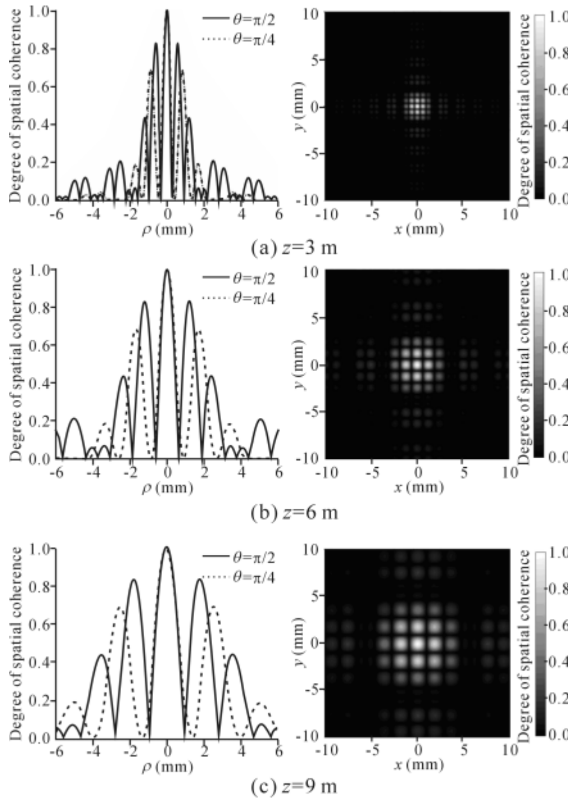

Fig.2 Spatial coherence distributions of the light field generated from a 2 × 2 multi-chip LED at three different observation planes

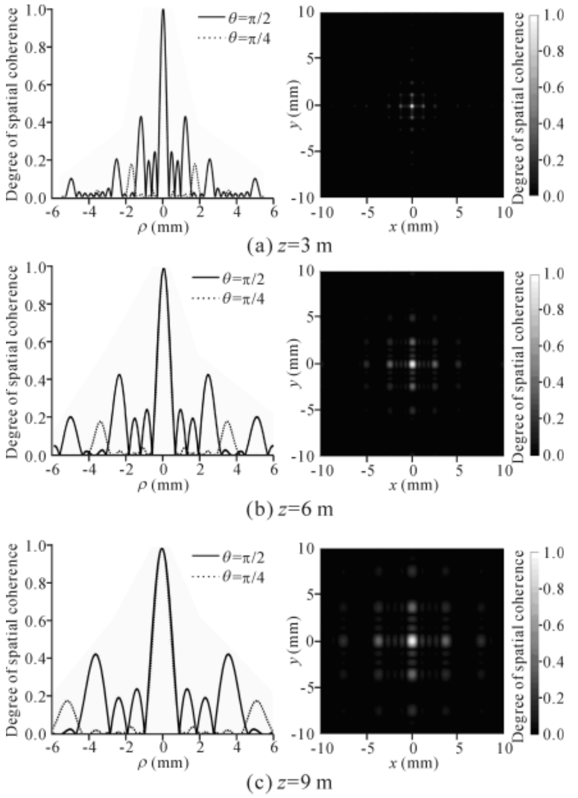

Fig.3 Spatial coherence distributions of the light field generated from a 4 × 5 multi-chip LED at three different observation planes

Theoretical calculations above show that the light generated from multi-chip LEDs evolves into the partially coherent light after propagation. The Young's double-slit interference experiment demonstrates a feasible method to measure the spatial coherence of the light. As shown in Fig.4, a multi-chip LED is connected to a heatsink, making the output power of the LED stable. The Young's double-slit is placed in the far zone (z=3 m), and the interference fringes are recorded by a CCD camera. Now we give some explanation to show how to measure the spatial coherence of the light field. Just as shown in Fig.4, the light from point P_1 and point P_2 can interfere with each other at CCD camera. We assume that the separation between two slits is L, and the light intensity at a point Q in the CCD detector plane is written as[15]

$$I(Q) = I_1(Q) + I_2(Q) + 2\sqrt{I_1(Q)I_2(Q)} \times |\mu_{12}(\omega)|\cos[\beta_{12}(\omega)] \quad , \tag{6}$$

where $I_1(Q)$ and $I_2(Q)$ are the intensities generated by two wavelets from point P_1 and point P_2, respectively, and $\mu_{12}(\omega)$ is the spectral coherence between point P_1 and point P_2, which is assumed to obey the quasi-monochromatic condition. $\beta_{12}(\omega)$ is the phase of $\mu_{12}(\omega)$ varying between 0 and 2π[9]. Traditionally, fringe visibility $V(Q)$ is determined by measuring the maximum (I_{max}) and minimum (I_{min}) of interference fringe intensity using following expression

$$V(Q) = \frac{I_{max} - I_{min}}{I_{max} + I_{min}} = \frac{2\sqrt{I_1(Q)I_2(Q)}}{I_1(Q) + I_2(Q)}|\mu_{12}(\omega)| \ . \tag{7}$$

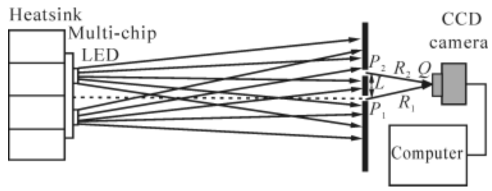

Fig.4 Schematic diagram of the experimental setup used for measuring the spatial coherence of the light generated from red multi-chip LEDs

With the assumption of $I_1(Q) = I_2(Q) = I(Q)$, Eq.(7) reduces to $V(Q)=|\mu_{12}(\omega)|$, from which the modulus of the degree of spectral coherence can be determined. Point P_1 is located on the optical axis. The spatial coherence of different points relative to the point on the optical axis can be measured by choosing different values of L. In our experiment, we choose six different values of L to fit the theoretical curve. Fig.5 shows the interference fringe distribution of the light generated from the 2×2 multi-chip LED with distance of z=3 m and different separations between two slits. One of the slits is fixed on the optical axis, while the distance of the other slit relative to the optical axis increases gradually along the radial direction. Fig.6 shows the interference fringe distribution of the light generated from the 4 × 5 multi-chip LED. The other experimental parameters are the same as those in Fig.5. In the

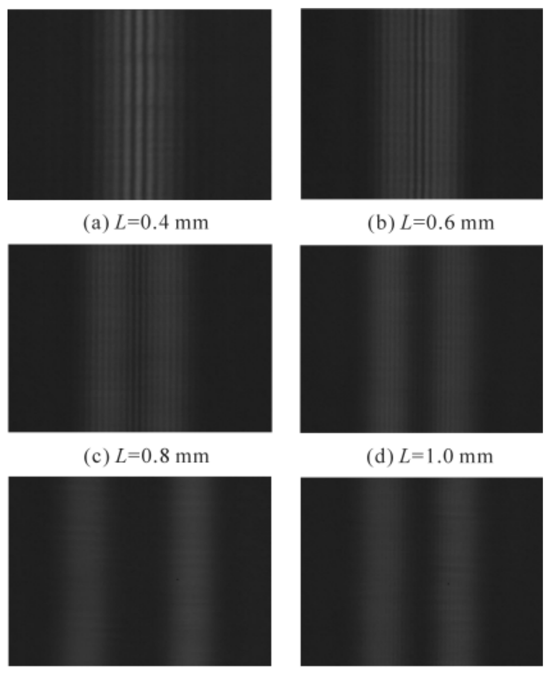

Fig.5 Double-slit interference fringes of the light irradiated from a 2 × 2 multi-chip LED with z = 3 m

double-slit interference experiment, we measure the interference fringe by a CCD and obtain the maximum (I_{max}) and minimum (I_{min}) of interference fringe intensity from a computer, so that we can get the modulus of the degree of spectral coherence. The distributions of the spatial coherences of the light generat- ed from 2 × 2 chip LED and 4 × 5 chip LED are shown in Fig.7(a) and (b), respectively. It is shown that the experimental results are consistent with the theoretical ones.

In conclusion, we theoretically and experimentally study the spatial coherence of two different types of high-power multi-chip red LEDs. It is shown that the light generated from multi-chip LEDs evolves into the partially coherent light after propagation, and the spatial coherence can be improved with increasing propagation distance. Based on the relationship between the spatial coherence and the interference fringe visibility, we experimentally measure the spatial coherence of the light generated from different types of multi-chip LEDs by double-slit interference experiment. The experimental observations agree with the theoretical simulations.

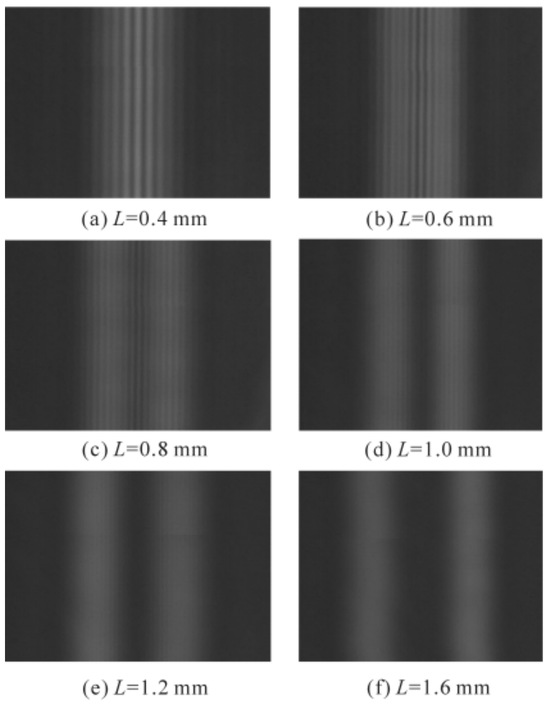

Fig.6 Double-slit interference fringes of the light irradiated from a 4 × 5 multi-chip LED with z=3 m

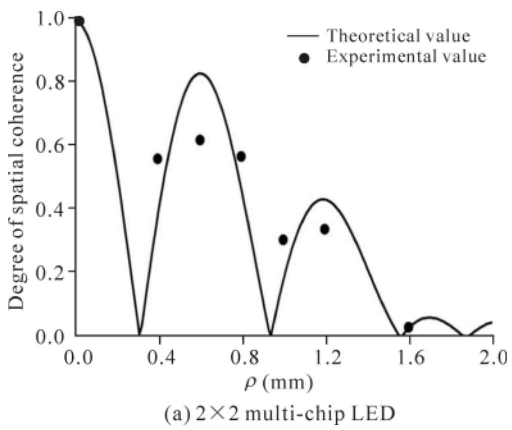

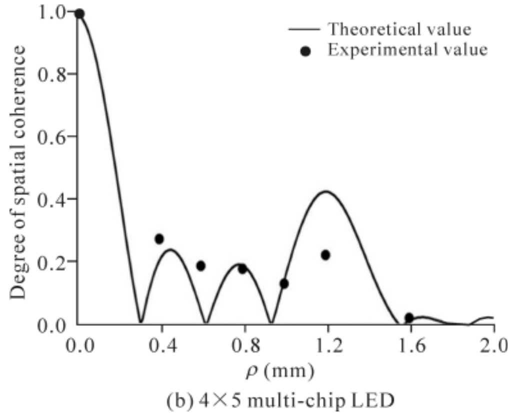

Fig.7 Distributions of spatial coherence of light field generated from two different multi-chip LEDs with z=3 m

References

[1] E. F. Schubert, Light-Emitting Diodes, Cambridge Univ. Press, UK, 2003.
[2] D. A. Steigerwald, J. C. Bhat, D. Collins, R. M. Fletcher, M. O. Holcomb, M. J. Ludowise, P. S. Martin and S. L. Rudaz, IEEE J. Sel. Top. Quantum Electron **8**, 310 (2002).
[3] J. Kim, S. Somani and Y. Yamamoto, Nonclassical Light from Semiconductor Lasers and LEDs, Spinger, 2001.
[4] S. Nakamura, T. Mukai and M. Senoh, Appl. Phys. Lett. **64**, 1687 (1994).
[5] M. G. Craford, N. Holonyak and F. A. Kish, Sci. Am. **284**, 63 (2001).
[6] Y. Narukawa, Opt. Photonics News **15**, 24 (2004).
[7] A. Bergh, G. Craford, A. Duggal and R. Haiz, Phys. Today **54**, 42 (2001).
[8] I. Moreno, C-C. Sun and R. Ivanov, Appl. Opt. **48**, 1190 (2009).
[9] Z. Guo, Y. Gao, Y. Lü, Y. Lin, H. Chen, R. Lei, Y. Chen and Z. Chen, Journal of Optoelectronics • Laser **22**, 992 (2011). (in Chinese)
[10] M. Peeters, G. Verschaffelt, H. Theinpont, S. K. Mandre, I. Fischer and M. Grabherr, Opt. Express **13**, 9337 (2005).
[11] M. Peeters, G. Verschaffelt, J. Speybrouck, H. Theinpont, J. Danckaert, J. Turunen and P. Vahimaa, Opt. Lett. **31**, 1178 (2006).
[12] F. J. Duarte, L. S. Liao and K. M. Vaeth, Opt. Lett. **30**, 3072 (2005).
[13] F. J. Duarte, Opt. Lett. **32**, 412 (2007).
[14] D. S. Mehta, K. Saxena, S. K. Dubey and C. Shakher, Journal of Luminescence **130**, 96 (2010).
[15] M. Born and E. Wolf, Principles of Optics, Cambridge Univ. Press, UK, 1999.
[16] MENG Zhuo, LIANG Yu, YAO Xiao-tian, YAO Hui, LIU Tie-gen and WAN Mu-sen, Journal of Optoelectronics • Laser **22**, 256 (2011). (in Chinese)
[17] Z. Chen, L. Hua and J. Pu, Prog. Opt. **57**, 219 (2012).